WARSAW UNIVERSITY OF TECHNOLOGY Index 351733
FACULTY OF CIVIL ENGINEERING
COMMITTEE FOR CIVIL AND WATER ENGINEERING
POLISH ACADEMY OF SCIENCES ISSN 1230-2945

DOI: 10.24425/ace.2021.138050

ARCHIVES OF CIVIL ENGINEERING

Vol. LXVII ISSUE 3 2021

s. 177–196



**Research paper**

# Wind tunnel model tests of wind action on the chimney with grid-type curtain structure

**A. Flaga[1], R. Kłaput[2], Ł. Flaga[3], P. Krajewski[4]**

**Abstract:** The subject of the wind tunnel tests is a steel chimney 85 m high of cylindrical – type structure with a grid-type curtain structure situated at its upper part. The model of the upper part of the chimney made in the scale of 1:19 was equipped with 3 levels of wind pressure measurement points. Each level contained 24 points connected with pressure scanners. On the base of the pressure measurements, both mean and instantaneous aerodynamic drag and side force coefficients were determined. Next wind gust factors for these two wind action components were determined. Moreover, for each pressure signal Fast Fourier Transform was done. Mean wind action components were also determined using stain gauge aerodynamic balance. Obtained results make possible to conclude that the solution applied in the upper part of the designed chimney is correct from building aerodynamics point of view. Some minor vortex excitations were observed during model tests of the upper part of the chimney. The basic dynamic excitation of this part of the chimney is atmospheric turbulence.

**Keywords:** model test, chimney with grid-type curtain, wind action, wind pressure determination

[1] Prof. Dr. Sc. Eng., Cracow University of Technology, Faculty of Civil Engineering, Wind Engineering Laboratory, Jana Pawła II 37/3a, 31-864 Cracow, Poland, e-mail: andrzej.flaga@pk.edu.pl, ORCID: https://orcid.org/0000-0002-9143-2014

[2] Dr. Eng., Cracow University of Technology, Faculty of Civil Engineering, Wind Engineering Laboratory, Jana Pawła II 37/3a, 31-864 Cracow, Poland, e-mail: renata.klaput@pk.edu.pl, ORCID: https://orcid.org/0000-0002-2631-1937

[3] Dr. Eng. Arch. Cracow University of Technology, Faculty of Civil Engineering, Wind Engineering Laboratory, Jana Pawła II 37/3a, 31-864 Cracow, Poland, e-mail: lukasz.flaga@pk.edu.pl, ORCID: https://orcid.org/0000-0001-9650-4913

[4] M.Sc. Eng., Cracow University of Technology, Faculty of Civil Engineering, Wind Engineering Laboratory, Jana Pawła II 37/3a, 31-864 Cracow, Poland, e-mail: piotr.krajewski2@pk.edu.pl, ORCID: https://orcid.org/0000-0002-2635-7273

# 1. Introduction

In order to evoke intensive lateral vibration of the structure due to vortex excitation, the following three main conditions should be fulfilled: 1. The critical wind velocity with regard to vortex shedding $V_{cr}^{v}$ should be for this structure within the range of possible wind velocities in the given territory; 2. The structure should be susceptible to vibration to such an extent as to permit the phenomenon of lock-in to occur i.e. the dimensionless parameter characterizing inertia and damping of this structure – e.g. Scruton number $Sc = \frac{2m\Delta}{\rho D^2}$ where: m -mass per structure unit length; $\Delta$ – logarithmic decrement of structure vibration damping; $\rho$ – air mass density; $D$ – cylined diameter or characteristics dimension of structure cross-section – should be possibly small. 3. The spatial-time structure of the onflowing air and the boundary conditions on the outer wall surface of the flow-round structure should be such as to permit fairy regular vortex formation and shedding in the vicinity of the lateral walls of this structure.

Hence, three basic reduction means of lateral vibration of the structure vortex shedding follow herefrom. These consist in: 1. Change of the critical wind velocity $V_{cr}^{v}$; 2. Increase of damping of vibration of the structure or/and its mass or/and application of vibration energy absorbers, called also mechanical vibration dampers (MVD); 3. Disturbance or even total elimination of vortex formation and their regular shedding. These may be achieved, in general, by two main measures: firstly, by changes in the structural properties (stiffness, mass and damping) and, secondly, by changes in the aerodynamic properties of the structure e.g.: changes in the whole geometry of the structure; addition of so called aerodynamic spoilers or turbulizers i.e. different aerodynamic appendages, protrusions, surface irregularities, changing the surface roughness; addition of different aerodynamic elements, changing the aerodynamic cross-sectional shape of the structure etc. These additional aerodynamic measures are commonly called aerodynamic vibration dampers (AVD).

Mechanical vibration dampers reduce the effects of vortex excitation (i.e. amplitude of lateral vibrations of the structure) and diminish also the feedback between the vibratin structure and the onflowing air, hence, in an indirect way they diminish the vortex excitation itself. It seems that the direct influence on the vortex source, i.e formation and shedding of vortices, is the more proper means of exerting influence on the vortex shedding effects. In other words, vibration of the structure excited by vortices can be effectively diminished or even totally eliminated by partial or complete make impossible of free vortex formation and their regular shedding from the structural

surface. For this purpose aerodynamic vibration dampers are used. Both AVD and MVD can be applied as passive or active dampers. In this paper only passive AVD will be spoken about.

A wide variety of aerodynamic appendages suppressing vortex excitation may be classified into the following three categories [1]: 1. Surface protrusions (strakes, helical wires, fins and studs, etc.), which destroy or reduce the coherence of the shed vortices by affecting separation lines and/or separated shear layers; 2. Shrouds (perforated, gauze, axial rods and axial slats, etc), which affect the entraint layers, and 3. Near wake stabilizers (splitter and saw-tooth plates, guiding plates and vanes, base-bleed, slits cut along the cylinder, etc.)which prevent interaction of entraint layers.

Most means in the first two categories mentioned above are irrespective of the direction of wind, whereas some means (1) and all in (3) are directional (e.g. uni-directional, two-directional). So, it depends on the given case which means in effective. Increase of drag coefficient in some of the above means should be also borne in mind.

Structures like chimneys are vulnerable to the vortex shedding phenomenon. These structures can reach large displacement amplitudes. Determination of the structural response is one of the most complicated problems in wind engineering. The effect of chimney vibration caused by vortex excitation has been reported in studies, e.g. [2, 3]. Different models for predicting the cross-wind response of cylindrical chimney, and tower shaped structures were presented e.g. in [4, 5, 6, 7].

An effective method of damping the vibrations can be to install a tuned mass damper (TMD). The effectiveness of the tuned mass damper (TMD) for vibration control were reported in [8], whereas the paper [9] focuses on the design of tuned liquid sloshing damper and compares this with the TMD. A simplified fluid structure interaction approach by using computational fluids dynamics were investigated in [10]. Many mathematical models in the field of vortex excitation have been elaborated. New approaches were presented in [11]. The paper [12] studied a cross-wind vibrations of a new steel chimney 100m high caused twice damage of bolts. Measured damping properties of the chimney permitted to compare different approaches to the calculation of relative amplitude of vibration. The paper [13] investigated the phenomenon of vortex-induced vibration through forced-vibration wind tunnel experiments on a rigid sectional model and on aeroelastic model that is free to oscillate under the wind action. The check of aerodynamic damping values obtained from the two experiments proves the effectiveness of the Vickery and Basu spectral model to predict vortex-induced vibrations. The paper [14] presents a collection of full-scale data selected from literature concerning measurements of cross-wind vibrations of chimneys. A novel spectral method was presented, whose predictions reproduce very well the oscillations measured in full-scale. The method is developed through wind tunnel tests in forced-vibrations. In turn the paper [15] compared

seven major international code methods for the design of reinforced concrete chimneys for across wind forces. The comparison of different important code provisions has been illustrated and evaluated with the help of three numerical example problems.

In publications concerning aerodynamic vibrations dampers (comp. e.g. [5, 16, 17, 18]) different structural solutions were discussed and results of investigations of the efficiency of various AVD were analysed. Some of the most frequently encountered solutions are presented collectively in Fig.1.

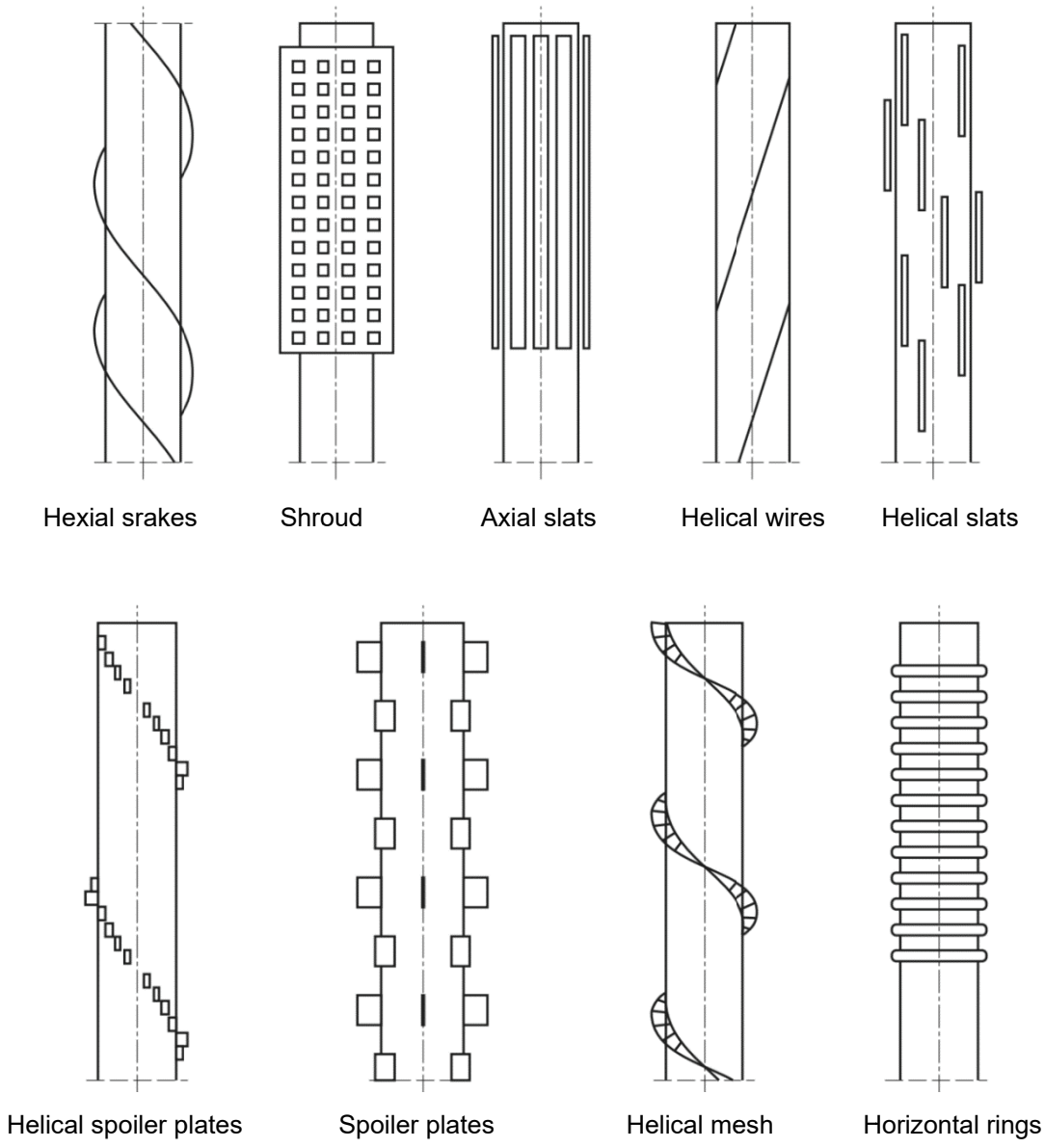


Fig. 1. Aerodynamic devices against vortex shedding applied for tower structures of circular cross-sections [5]

Basing on observations in wind tunnels and investigations in natural scale, it may be stated that, in spite of AVD mounted on the structure, the vortex street can be formed at a distance of about (4–6) $D$ behind the structure, and, moreover, at lateral vibration of the structure greater than $0.2D$ the vortex street is almost identical as in the case of absence of AVD. This phenomenon is of significant meaning for leeward structures located in the wake of the windward structure. It results from the investigations that, in spite of the application of AVD, a leeward structure can be subjected to an intensive vortex excitation. AVD are efficient in such cases when the distance between the objects is greater than $10D$.

Also in the case of a structure highly susceptible to vibration (i.e.of low $Sc$ number), AVD can be completely inefficient. This usually refers to structure od $Sc \leq 6–8$ [16]. In these cases, lateral vibration of an amplitude level greater than $0.05D$ (caused by e.g. random fluctuations of wind velocity and wind direction) can be easily excited and this is already sufficient to form a vortex street behind the object, a street similar to such one as in the case of AVD absence.

The strake or shroud to be effective must extend into the region where the maximum excitation originates. For tapered structures this may require it to be extended lower than $H/3$ from the tip and, for stepped structures, strakes or shrouds may be required on the lower sections as well as or, sometimes instead of the upper, smallest-diameter section.

Some spoilers increase the mean drag coefficient which will lead to increased buffeting response and those which introduce asymmetry into the structural cross-section may lead to problems with response due to galloping.

Majority of the presented investigations results refer to model investigations in wind tunnels in the subcritical range of $Re$ number. In other Re number ranges, it may be provided that the discussed solutions of AVD are either less and less or even not at all efficient or have other properties than in the subcritical range of $Re$ number. Little is also known about the influence of the vertical wind profile $V(z)$, and especially about the influence of the fluctuation intensity of wind velocity $I_v$. This, however, requires verification and further comprehensive studies and investigations, mainly in natural scale.

Mathematical modelling of vortex-induced excitation of structure fitted with spoilers is an open problem (comp. e.g. [5, 18]).

The original solution of vortex excitation suppressing in the case of nontypical steel chimney 120 m height was elaborated and investigated in natural scale by [18]. In this solution together TMD and AVD dampers were used effectively.

The paper aims of the wind tunnel model tests of a cylindrical-type stell chimney 85 m high equipped with a grid type curtain structure situated at its upper part to reduce mainly vortex-induced excitation and vibration of the chimney. The grid-type curtain structure situated in the upper part of cylindrical chimney is a new solution of the analysed issue elaborated by Steelcon Chimney Company, Cracow Division, Poland. So, wind action on the upper part of such chimney had to be determined during design process of the chimney. To resolve this problem, tests of the upper part of the chimney were performed in a boundary layer wind tunnel of the Wind Engineering Laboratory at the Cracow University of Technology, Poland. On the base of the pressure measurements, both mean and instantaneous aerodynamic drag and side force coefficients were determined. Next wind gust factors for these two wind action components were determined. Moreover, for each pressure signal Fast Fourier Transform was done. Mean wind action components were also determined using stain gauge aerodynamic balance.

# 2. Wind tunnel setup

## 2.1. Aerodynamic model

Aerodynamic model of the designed structure was made in the scale of 1:19. Sectional model includes the upper part of the chimney with the grid-type curtain structure (see Fig. 2). A mass tuned damper is designed in the upper part of the chimney, within the protective mesh. It is the most suitable scale for this structure due to the overall size of the chimney, the size of grid, the dimensions of the wind tunnel working section, and the required scope for structure modelling. The model was equipped with 3 levels of wind pressure measurement points. Each level contained 24 points connected with pressure scanners. The model was fixed to the strain gauge aerodynamic balance.

The shaft of the test model was made of Ø150 mm PVC pipe with a wall thickness of 4 mm. Some parts of the core (mass damper and chimney outlet) were made in 3D printing technology from ABS material. Then those parts were polished to obtain a smooth surface. The grid-type curtain structure was made of steel sheet of 3mm thickness, cut with laser and bent to Ø275 mm diameter. The platforms and the mounting base for the strain gauge aerodynamic balance were made of steel sheet. Then the elements were cut using a precision method on the turning lathe. Trapezoidal cantilevers were made of foamed PVC of 3 mm thickness.

The model was geared with measuring systems. Steel micro-tubes inlets of measurement points (pressure taps) were placed on elevation surfaces. This will allow for measurement external pressure distributions caused by wind. Measurement points were connected with pressure scanners via a set of tubes. These scanners were located inside the chimney. Arrangement of the measurement points are presented in Fig. 3.

a) b)

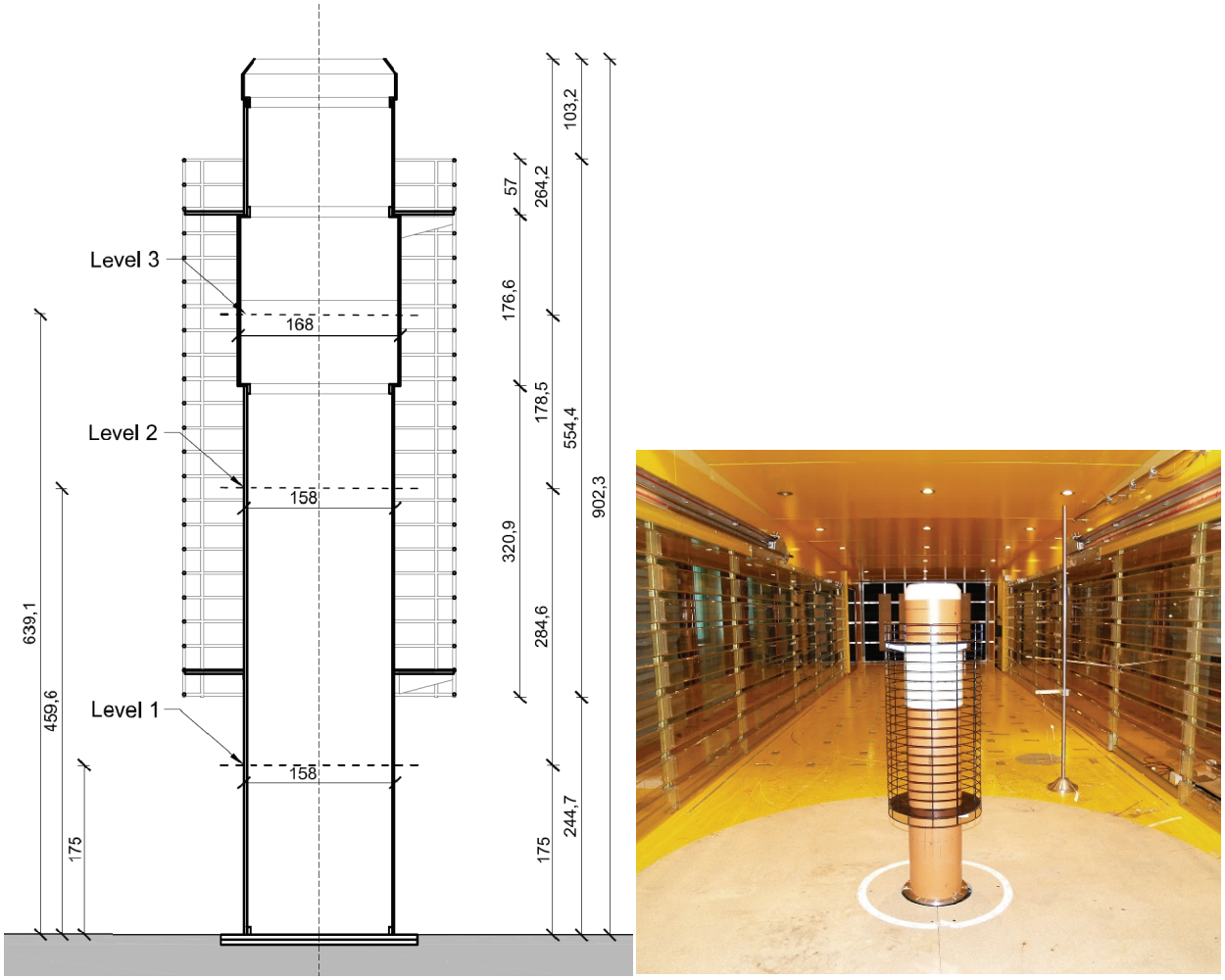


Fig. 2. The vertical cross – section of the chimney sectional model with the grid-type curtain structure made in the scale of 1:19 (a); the sectional model in the wind tunnel working section; view from leeward wind direction (b)

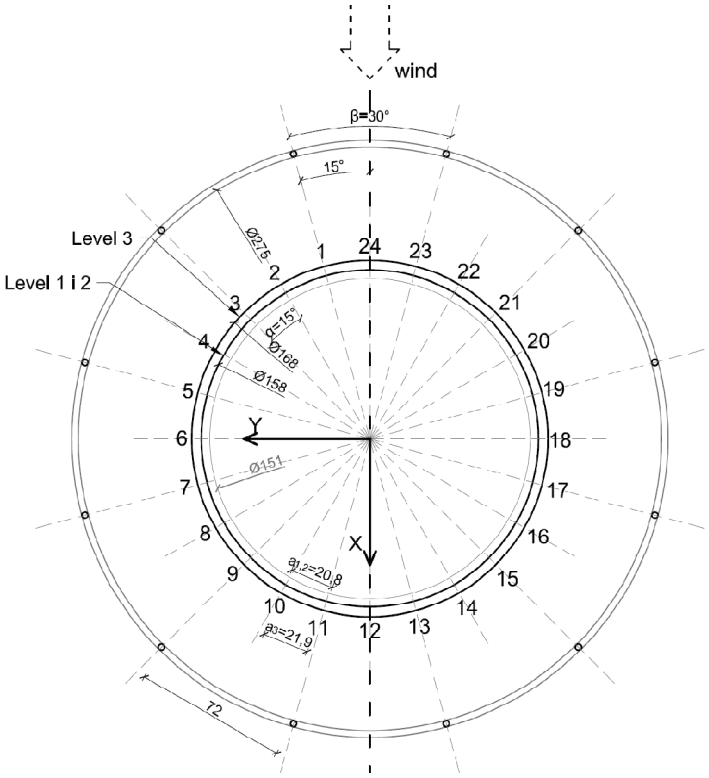


Fig. 3. Arrangement of the measurement points (measurement point numbers) in relation to the direction of onflowing wind

## 2.2. Wind structure

In the preliminary stage of the tests, the flow pattern inside the working section of the wind tunnel was determined. The assumptions for flow pattern determination referred to wind conditions in the location of the planned structure. The flow pattern was formed with special modifying elements in the form of a turbulising grid (see Fig. 4). The flow pattern inside the working section of wind tunnel was measured using pressure scanners. The turbulence intensity measured in front of the model in undisturbed air onflow was 16%. The sectional model of chimney was located in last segment of wind tunnel working section. Sampling frequency for each measurement was 200 Hz.

The scope of sectional model referred to the top of the chimney, which is situated at 85m above surrounding ground level. For such altitude wind profile shows slight differences in values. Due to this fact wind structure recreated within the wind tunnel for this experimental test was uniform along z axis for both velocity and turbulence intensity level.

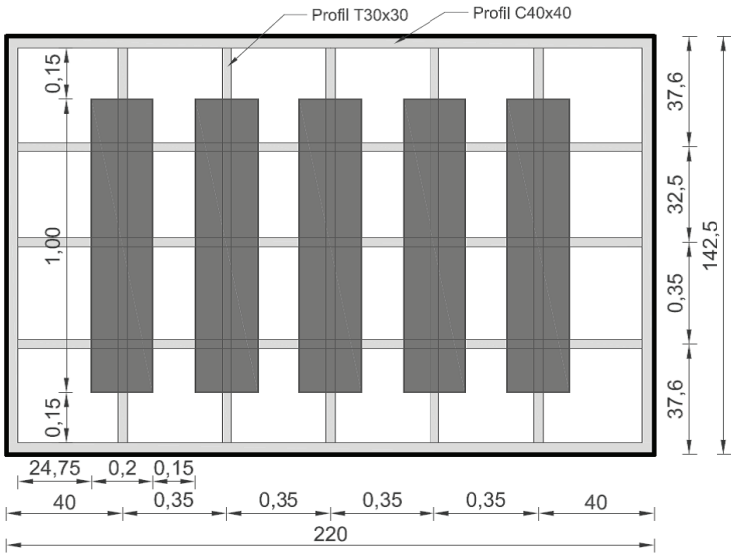


Fig.4. Turbulising grid forming a turbulence inside the wind tunnel; drawing with basic dimensions of each element

# 3. Basic denotations and definitions

## 3.1. Wind pressure measurements

On the basis of wind pressure with values received from the model tests, the following aerodynamic coefficients were specified:

(3.1) $$w_{jk} = \sum_{i=1}^{24}\left(p_i f_j(\alpha_i)\right) l_i = w_{jk}(t);$$

(3.2) $$w_{jk}(t) = \frac{1}{2}\rho \bar{V}_{ref}^2 C_{jk}(t) d_k;$$

(3.3) $$f_j(\alpha_i) = \begin{cases} \sin\alpha_i & \text{when } j = x \\ \cos\alpha_i & \text{when } j = y \end{cases}$$

where: $C_{jk}(t)$ - aerodynamic coefficient as a function of time $t$ (see Fig 5)

(3.4) $$C_{jk}(t) = \frac{2}{\rho \bar{V}_{ref}^2 d_k} \sum_{i=1}^{24}\left(p_i f_j(\alpha_i)\right) l_i;$$

(3.5) $$C_{jk} = \overline{C_{xk}}(t) = \frac{1}{T}\int_0^T C_{jk}(t)\mathrm{dt}\,;$$

(3.6) $$C'_{jk}(t) = C_{jk}(t) - \overline{C_{jk}}(t)$$

(3.7) $$\beta_{jk} = \frac{C_{jk}^{\max}}{C_{jk}}.$$

where: $w_{jk}$ – $j$-component of aerodynamic force acting on the model; $j = x, y$, $k = 1, 2, 3$ – level of measurement points, $i$ – pressure tap number, $x$ – along – wind direction, $y$ – across-wind direction, $C_{jk}$ – mean pressure coefficient, $p_i$ – wind pressure measured in point $i$ of polar angle $\alpha_i$; $d_i$ –

diameter of the cross-section; $l_i$ – the peripheral length of the segment (Fig. 6); $T$ – averaging time; $\beta_{jk}$ – wind gust action factors for component $j = x, y$.

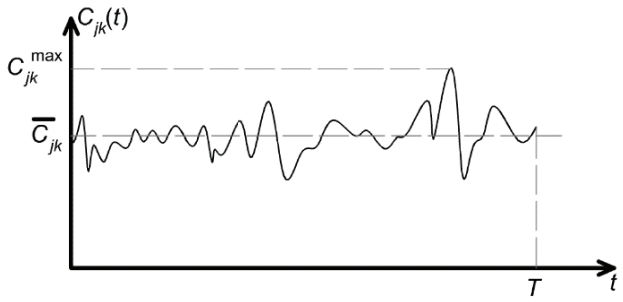


Fig. 5. Sample time course of the coefficient $C_{jk}(t)$ obtained from wind pressure measurement and its characteristic values: $\overline{C_{jk}}$, $C_{jk}^{\max}$; $\beta_{jk} = \frac{C_{jk}^{\max}}{C_{jk}}$; where: $j = x, y$; $k$ = 1,2,3 (level number according to Fig.2); $T$ – averaging time

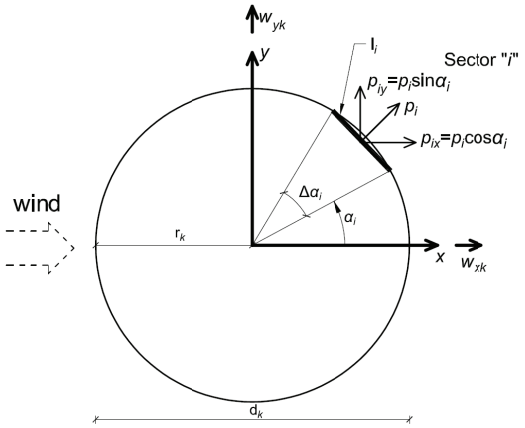


Fig. 6. Diagram of geometrical and mechanical quantities defining aerodynamic drag force and aerodynamic side force

## 3.2. Aerodynamic balance measurements

On the basis of the fixing aerodynamic forces the following aerodynamic coefficients were specified:

$$w_x(t) = \frac{1}{2}\rho\bar{V}_{ref}^2 C_x(t)d \tag{3.8}$$

where: $C_x(t)$ – aerodynamic coefficient as a function of time $t$ (see Fig 7), $w_x$ – $x$ component of aerodynamic force acting along – wind direction;

(3.9) $$C_x(t) = C_x + C'_x(t)$$

(3.10) $$C_x = \frac{1}{T}\int_0^T C_x(t)\mathrm{dt}$$

(3.11) $$C'_x(t) = C_x(t) - C_x$$

where: $d$ – assumed as 0,168m (diameter on level 3 - mass damper)

(3.12) $$w_y(t) = \frac{1}{2}\rho\bar{V}_{ref}^2 C_y(t)d$$

where: $C_y(t)$ – aerodynamic coefficient as a function of time $t$ , $w_y$ – $y$ component of aerodynamic side force acting across – wind direction.

(3.13) $$C_y(t) = C_y + C'_y(t)$$

(3.14) $$C_y = \frac{1}{T}\int_0^T C_y(t)\mathrm{dt}$$

(3.15) $$C'_y(t) = C_y(t) - C_y$$

where: $d$ – assumed as 0,168m (diameter on level 3 - mass damper)

In both wind tunnel tests of measured quantities and in this study, the following denotations and definitions were used:

(3.16) $$q_{ref} = \frac{1}{2}\rho V_{ref}^2$$

$q_{ref}$ – reference wind velocity pressure: mean value of dynamic wind pressure of onflowing air in front of the model; where: $\rho$ – atmospheric air density; $V_{ref}$ – average reference horizontal flow speed at reference height.

Surface roughness of the model was adopted as for steel plate i.e. $k/D = 0{,}001$. For the range of velocities performed (6,1-19,3m/s) the range of $Re$ number was obtained: $6{,}47 \cdot 10^4 - 2{,}04 \cdot 10^5$, according to formula:

(3.17) $$Re = \frac{V \cdot \mathrm{D}}{\nu}$$

where: $V$ – mean velocity of oncoming air ($\frac{m}{s}$), $\nu$ – kinematic viscosity $1.5 \cdot 10^{-5}$ [$\frac{m^2}{s}$] for 20°C, for characteristic dimension of chimney model core $D = 0{,}159$ m.

Dynamic analysis of the chimney indicated values of frequencies for 3 active modes: 1st mode 0,39 [Hz], 2nd mode 2,03 [Hz] and 3rd mode 5,53[Hz]. Basing on [20] for circular cylinder, the value of $St = 0{,}21$ was adopted for $V_{cr}^V$ calculation:

(3.18) $$V_{cr}^V = \frac{f_v \cdot \mathrm{D}}{St}$$

where: $V_{cr}^v$ – critical velocity of vortex excitation [$\frac{m}{s}$], $f_v$– frequency of vortex shedding [Hz], $D = 2.9$ [m] characteristic dimension of the chimney core.

Critical velocities of onflowing air for the chimney are respectively: $V_{cr\,1}^{v} = 5{,}6\,[\frac{m}{s}]$, $V_{cr\,2}^{v} = 29{,}4\,[\frac{m}{s}]$ and $V_{cr\,3}^{v} = 80{,}1\,[\frac{m}{s}]$. Critical frequencies of each mode for adopted modelling scale result from dimensional analysis dependency:

$$k_f = \frac{1}{k_t} = \frac{k_v}{k_D} \tag{3.19}$$

where: $\frac{k_f}{t}$ – scale of frequency, $k_v$ – scale of velocity $[\frac{m}{s}]$, $k_D$- scale of geometry [m].

According to formula (6.19) critical frequencies of each mode in model scale are respectively: 7.38 [Hz], 38.58 [Hz] and 105.01 [Hz]. One should notice that the first and the second one is of greater importance due to range of corresponding velocities occurring more frequently within the location of the chimney.

Wind tunnel tests were performed with the set of velocities of oncoming air in the range of 6,1–19,3 m/s. There is a relationship between velocity of oncoming air and the level of frequency (band of frequencies) of vortex excitation for circular cylinder given by formula:

$$f_v = \frac{St \cdot V_{ref}}{\mathrm{D}} \tag{3.20}$$

The set of frequencies of vortex excitation $f_v$ corresponding to reference velocity $V_{ref}$ of oncoming air and characteristic dimension $D$ is presented in Tab. 1. These values were indicated on particular diagrams in chapter 4 (see Figs. 6–10).

Table 1. Set of frequencies of vortex excitation $f_v$ corresponding to reference velocity $V_{ref}$ of oncoming air and characteristic model dimension $D_{mod}$

| $D_{mod}$ [m] | $V$ [m/s] | 6.1 | 11.1 | 13.7 | 15.6 | 18.8 | 19.3 |
|---|---|---|---|---|---|---|---|
| 0.158 | $f_v$ [Hz] | 8.11 | 14.75 | 18.21 | 20.73 | 24.99 | 25.65 |
| 0.168 | | 7.63 | 13.88 | 17.13 | 19.50 | 23.50 | 24.13 |

# 4. Results of wind tunnel model tests

## 4.1. Results of the wind pressure model tests on the external surface of the chimney

The measurement aims at the determination of pressure distribution in each measurement point $p_i$ [Pa] in relation to the direction of onflowing wind for three measurement levels (level 1, 2 and 3). During wind tunnel tests wind velocity was increased by manually controlling the frequency

rotation of the fan. At first, the velocity was stabilized at about 6.1 m/s, and then it was increased up to 19.3 m/s with adopted transitional values. On the base of the pressure measurements, both mean and instantaneous aerodynamic drag and side force coefficients were determined. Next wind gust factors for these two wind action components were determined. Results of aerodynamic coefficients $C_{jk}$ and wind gust action factors $\beta_{jk}$ for all measurement levels are presented in Tab.2. Moreover, for each pressure measurement signal Fast Fourier Transform module was done.

Table 2. Values of aerodynamic coefficients $C_{jk}$ and wind gust factors $\beta_{jk}$ for 1, 2, 3 measurement levels.

| Points 1–24, $d_k$ = 0.158 m (level 1), $l_i = 0.0208$ | | | Wind gusts action coefficient |
|---|---|---|---|
| $V_{ref}$ [m/s] | $C_{xk}$ | $C_{yk}$ | β |
| 6.1 | 0.66 | 0.03 | 2.93 |
| 11.1 | 0.61 | 0.06 | 11.1 |
| 13.7 | 0.62 | 0.07 | 2.88 |
| 15.6 | 0.61 | 0.08 | 2.81 |
| 18.8 | 0.63 | 0.08 | 2.84 |
| 19.3 | 0.64 | 0.08 | 2.88 |
| Points 25–48, $d_k$ = 0.158 m ( level2), $l_i = 0.0208$ | | | |
| $V_{ref}$ [m/s] | $C_{xk}$ | $C_{yk}$ | β |
| 6.1 | 0.49 | 0 | 3.25 |
| 11.1 | 0.41 | –0.01 | 11.1 |
| 13.7 | 0.42 | –0.01 | 3.23 |
| 15.6 | 0.43 | –0.01 | 3.03 |
| 18.8 | 0.44 | –0.01 | 2.97 |
| 19.3 | 0.44 | –0.01 | 2.99 |
| Points 49–72, $d_k$ = 0.168 m (level 3), $l_i = 0.0219$ | | | |
| $V_{ref}$ [m/s] | $C_{xk}$ | $C_{yk}$ | β |
| 6.1 | 0.51 | 0.01 | 2.41 |
| 11.1 | 0.48 | 0 | 11.1 |
| 13.7 | 0.49 | 0 | 2.86 |
| 15.6 | 0.50 | –0.01 | 2.64 |
| 18.8 | 0.51 | –0.01 | 2.62 |
| 19.3 | 0.52 | –0.02 | 2.72 |

On the basis of the results obtained in the wind tunnel, the following remarks can be noticed: the highest aerodynamic coefficients appears in level 1 and is equal to above 0.6. In the upper part of the chimney, within the protective mesh the value of aerodynamic coefficiets are slightly lower. The

spectra of Fast Fourier Transform (FFT) module obtained from pressure measurements are presented in Fig. 7–11.

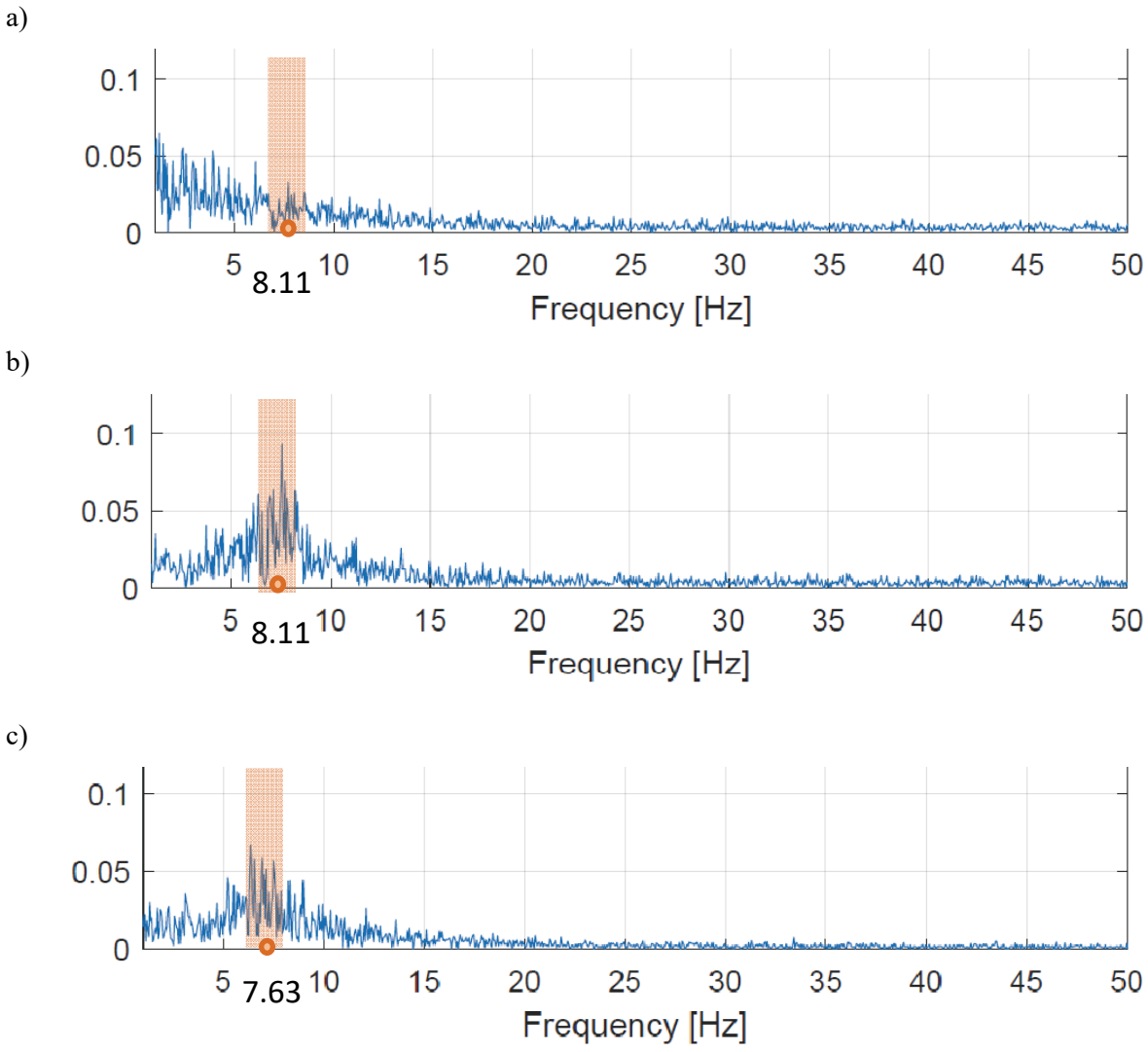


Fig. 7. Fast Fourier Transform (FFT) module spectra for across wind force $w_y(t)$ obtained from pressure measurements at onflowing velocity 6.1 m/s: level 1 (a), level 2 (b) & level 3 (c)

Analysis of FFT module spectra of side force $w_y(t)$ at onflowing velocity 6.1 m/s shows local peak for band of mean frequency at 7.55 Hz, which match to vortex excitation $f_v$ values (see Tab. 1). However level of this excitation is rather low (see Fig. 8).

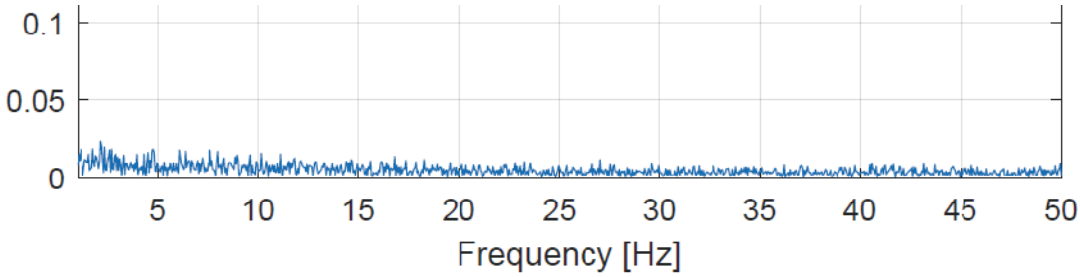


Fig. 8. Fast Fourier Transform (FFT) module spectrum for along wind force $w_x(t)$ obtained from pressure measurements at onflowing velocity 6.1 m/s level2

a)

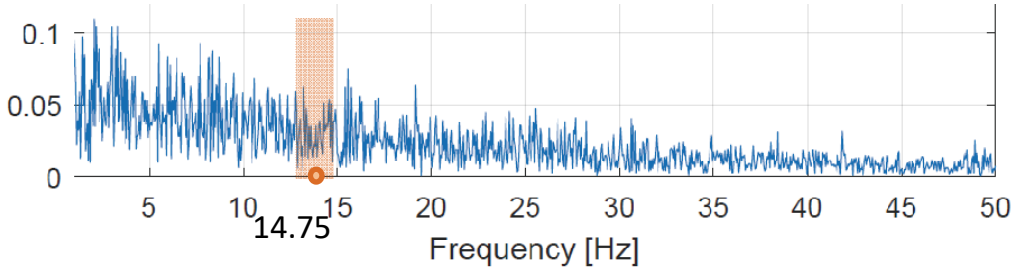


b)

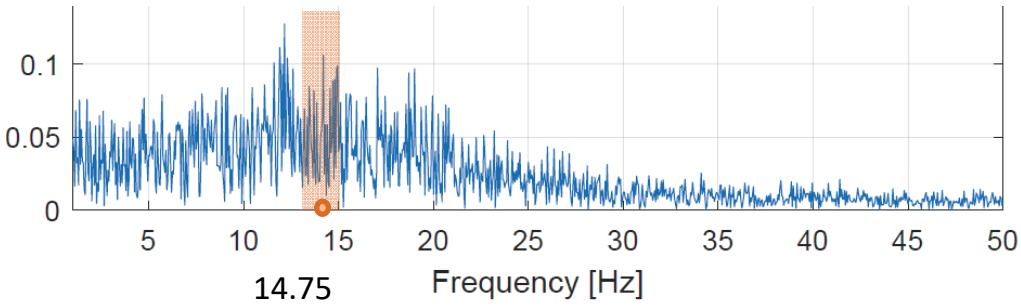


c)

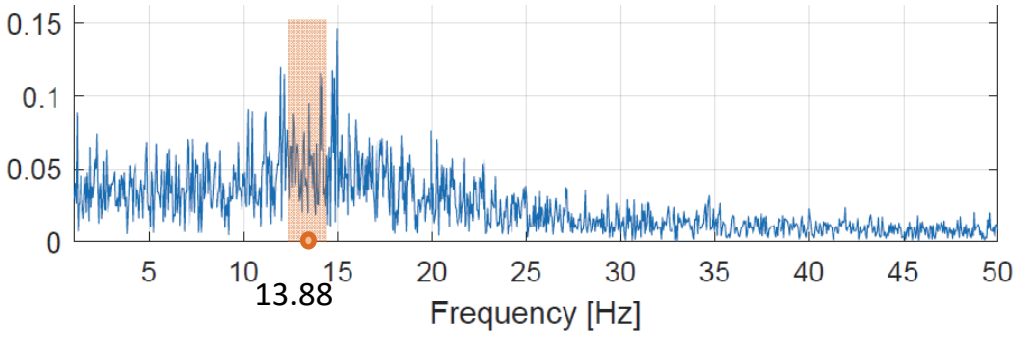


Fig. 9. Fast Fourier Transform (FFT) module spectra for across wind force $w_y(t)$ obtained from pressure measurements at onflowing velocity at 11.1 m/s: level 1 (a), level 2 (b) & level 3 (c)

a)

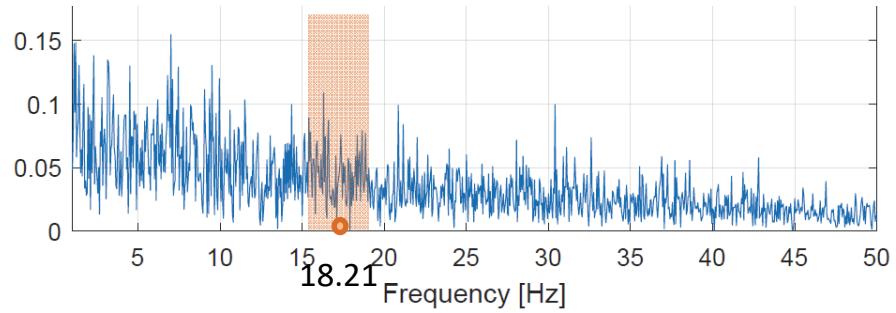


b)

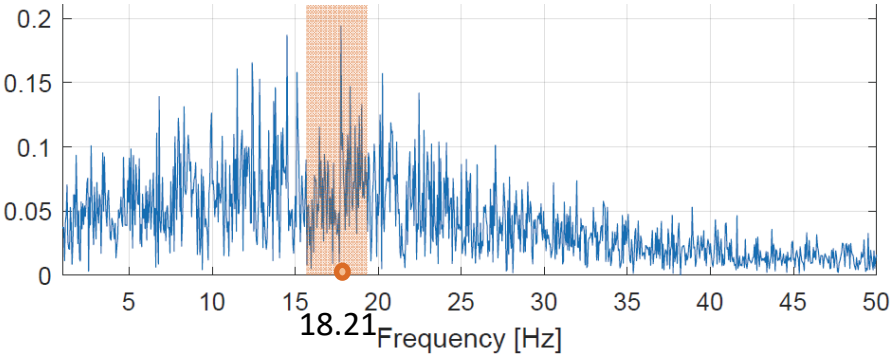


c)

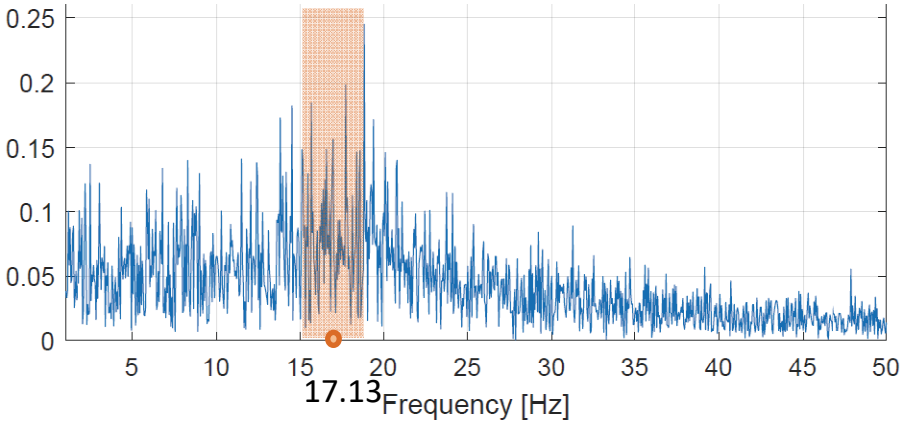


Fig. 10. Fast Fourier Transform (FFT) module spectra for across wind force $w_y(t)$ obtained from pressure measurements at onflowing velocity at 13.7 m/s: level 1 (a), level 2 (b) & level 3 (c)

Analysis of FFT module spectra of $w_y(t)$ lift force at onflowing velocity 13.7 m/s shows that local peak for band of mean frequency at around 17–18 Hz $f_v$ values fades away (see Tab. 1). This phenomena escalates at higher wind velocities, when local peak vanishes within signal recorded (see Fig. 10). One should also notice that signal at these velocities show lots of local peak values at whole spectrum, which is a result of – among others - small vortex generating by the grid type curtain structure.

a)

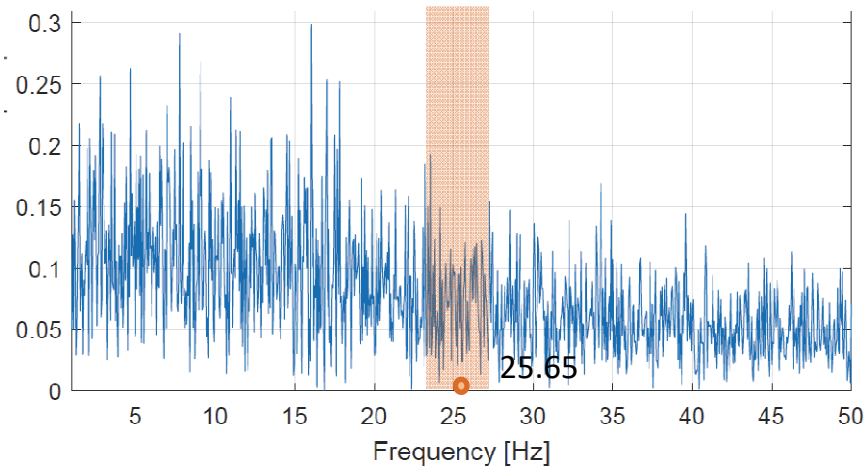


b)

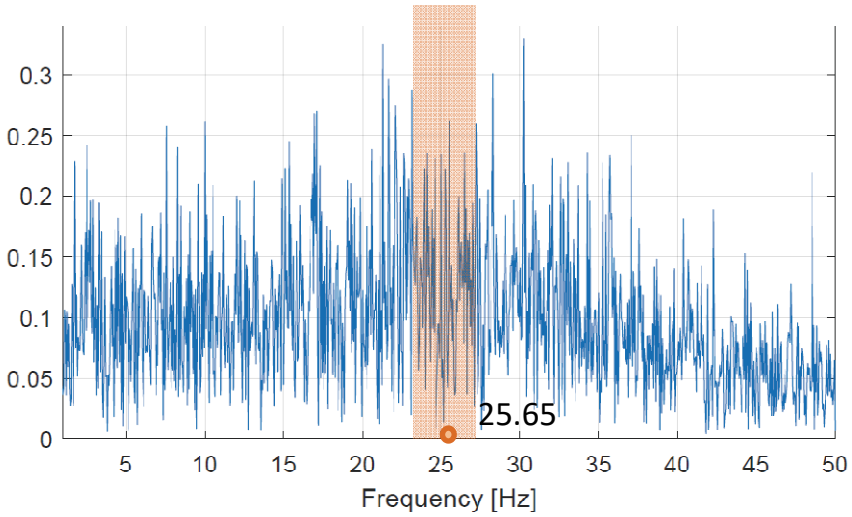


c)

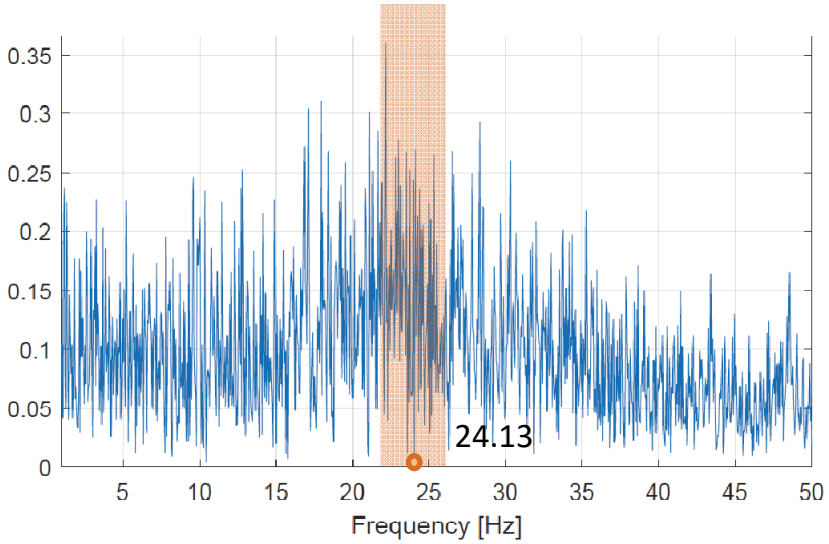


Fig. 11. Fast Fourier Transform (FFT) module spectra for across wind force $w_y(t)$ obtained from pressure measurements at onflowing velocity 19.3 m/s: level 1 (a), level 2 (b) & level 3 (c)

For each adopted velocity of oncoming air, the frequency of vortex excitation $-f_v$ was indicated (see Figs 6–10). The scope of velocities (6.0–19.3 m/s) is not "covering" full range of corresponding frequencies, however it is sufficient to prove efficiency of tested grid-type curtain structure. Based on results obtained some vortex excitation phenomena takes place within grid-type curtain structure surroundings. Analysis of FFT module of lift force $w_y(t)$ obtained from pressure measurements for *y* direction (across the direction of onflowing air) shows local extreme values for bands of mean frequency value corresponding to vortex excitation $f_v$. This phenomena is more easy to notice for lower velocities of oncoming air, for which the band of frequencies is tight and the peak emphasizes. The higher the wind velocity is the wider the band becomes and peak vanishes in the overall signal structure. Furthermore for higher wind velocities the signal represents lots of tight peaks which are representing vortexes generated by the curtain grid structure. Base on this analysis one can stated that the structure has a beneficial influence to the flow pattern around chimney top section.

## 4.2. Aerodynamic forces test results obtained from strain gauge aerodynamic balance

Additional measurements of aerodynamic forces and moments acting on the model were conducted as well. They were carried out using strain gauge aerodynamic force balance. Coefficients of two mean aerodynamic forces were measured during the tests on the aerodynamic balance: $F_x$ – mean aerodynamic drag force, $F_y$ – aerodynamic side force. The model was stiffly fixed to the aerodynamic balance. The measurements were carried out for a few mean wind velocities.

The values of mean aerodynamic forces $F_x$ and aerodynamic coefficients $C_x$& $C_y$, obtained from strain gauge aerodynamic balance are presented in Tab. 3.

Table 3. The values of mean aerodynamic forces $F_x$ and aerodynamic coefficients $C_x$& $C_y$ and a corresponding *Re* number

| $V_{ref}$ [m/s] | $F_x$ [N] | $C_x$ | $C_y$ | Re |
|---|---|---|---|---|
| 6.1 | 2.9 | 0.82 | –0.02 | $6.47 \cdot 10^4$ |
| 13.7 | 14.3 | 0.82 | –0.02 | $1.44 \cdot 10^5$ |
| 15.6 | 18.6 | 0.82 | –0.01 | $1.65 \cdot 10^5$ |
| 18.8 | 27.8 | 0.85 | –0.02 | $1.99 \cdot 10^5$ |
| 19.3 | 29.4 | 0.85 | –0.01 | $2.04 \cdot 10^5$ |

# 5. Summarise and final remarks

The solution applied in the upper part of the designed chimney is correct, from building aerodynamics point of view. Some minor vortex excitations were observed during model tests of the upper part of the chimney. The basic dynamic excitation of this part of the chimney is atmospheric turbulence. There are quite significant differences in the mean values of aerodynamic coefficients obtained from pressure distribution measurements and from strain gauge aerodynamic balance. The reason for this is that the values of aerodynamic coefficients obtained from pressure distribution measurements refer to three different local areas (1,2 &3 level) separately. The values of aerodynamic coefficients obtained from the strain gauge aerodynamic balance refer to the entire section of tested chimney, which also include local effects of a different flow pattern around the chimney top (so called tip effect). One should also note that there are different reference diameter values ($d_k$ – for pressure distribution measurements & $d$ – for strain gauge aerodynamic balance measurements) in the definitions of aerodynamic coefficients.

**Acknowledgements:**

This paper was elaborated basing on commissioned work funded by Steelcon Chimney Esbjerg A/S 62

## References

[1] Zdravkovich M.M., "Review and classification oof various aerodynamic and hydrodynamic means for suppressing vortex shedding". J.Wind Eng. Ind. Aerodyn., 7(2): pp. 145-189, 1981.

[2] Arunachalam, S., & Lakshmanan, N. (2015). "Across-wind response of tall circular chimneys to vortex shedding". *Journal of Wind Engineering and Industrial Aerodynamics, 145*, pp. 187–195, https://doi.org/10.1016/j.jweia.2015.06.005.

[3] Wang, L., & Fan, X. (2019). "Failure cases of high chimneys: A review". *Engineering Failure Analysis*, *105*, pp. 1107–1117, https://doi.org/10.1016/j.engfailanal.2019.07.032.

[4] Vickery, B. J., & Basu, R. I., "The response of reinforced concrete chimneys to vortex shedding". *Engineering Structures*, *6*(4), pp. 324–333, 1974

[5] Flaga A., "Wind vortex-induced excitation and vibration of slender structures-single structure of circular cross-section normal to flow". Monograph No. 202. Cracow University of Technology, Cracow 1996.

[6] Lipecki, T., & Flaga, A. (2013). "Vortex excitation model. Part I. mathematical description and numerical implementation". Wind and Structures, 16(5), pp. 457–476.

[7] Lipecki, T., & Flaga, A. (2013). "Vortex excitation model. Part II. application to real structures and validation". Wind and Structures, 16(5), pp. 477–490, https://doi.org/10.12989/was.2013.16.5.477.

[8] Brownjohn, J. M. W., Carden, E. P., Goddard, C. R., & Oudin, G. (2010). "Real-time performance monitoring of tuned mass damper system for a 183 m reinforced concrete chimney". *Journal of Wind Engineering and Industrial Aerodynamics*, *98*(3), pp. 169–179, https://doi.org/10.1016/j.jweia.2009.10.013.

[9] Christensen, R. M., Nielsen, M. G., & Støttrup-Andersen, U. (2017). "Effective vibration dampers for masts, towers and chimneys". *Steel Construction*, *10*(3), pp. 234–240, https://doi.org/10.1002/stco.201710032.

[10] Belver, A. V., Ibán, A. L., & Lavín Martín, C. E. (2012). "Coupling between structural and fluid dynamic problems applied to vortex shedding in a 90m steel chimney". *Journal of Wind Engineering and Industrial Aerodynamics*, *100*(1), pp. 30–37. .

[11] Verboom, G. K., & van Koten, H. (2010). "Vortex excitation: Three design rules tested on 13 industrial chimneys". *Journal of Wind Engineering and Industrial Aerodynamics*, *98*(3), pp. 145–154, https://doi.org/10.1016/j.jweia.2009.10.008.
[12] Kawecki, J., & Żurański, J. A. (2007). "Cross-wind vibrations of steel chimneys – A new case history". *Journal of Wind Engineering and Industrial Aerodynamics*, *95*(9–11), pp. 1166–1175.
[13] Lupi, F., Höffer, R., & Niemann, H.-J. (2021). "Aerodynamic damping in vortex resonance from aeroelastic wind tunnel tests on a stack". *Journal of Wind Engineering and Industrial Aerodynamics*, *208*, pp. 104–438.
[14] Lupi, F., Niemann, H.-J., & Höffer, R. (2017). "A novel spectral method for cross-wind vibrations: Application to 27 full-scale chimneys". *Journal of Wind Engineering and Industrial Aerodynamics*, *171*, pp. 353–365, https://doi.org/10.1016/j.jweia.2017.10.014.
[15] Rahman, S., Jain, A. K., Bharti, S. D., & Datta, T. K. (2020). "Comparison of international wind codes for across wind response of concrete chimneys". *Journal of Wind Engineering and Industrial Aerodynamics*, *207*, pp. 104–401.
[16] Ruscheweyh H., "Dynamische Windwirkung an Bauwerken. Band 2: Praktische Anwendungen. Bauverlag". Wiesbaden und Berlin, 1982.
[17] Blevins R.D., "Flow-induced vibration. Second edition". Van Nostrand Reinhold, New York 1990.
[18] Flaga A., "Wind engineering – fundamentals and applications" (in Polish), Arkady, Warsaw (2008).

## Badania modelowe oddziaływania wiatru na komin z konstrukcją siatki osłonowej

**Słowa kluczowe:** badanie modelowe, komin z kurtyną kratową, oddziaływanie wiatru, wyznaczanie ciśnienia wiatru

**Streszczenie:**

Przedmiotem badań w tunelu aerodynamicznym był stalowy komin wysokości 85 m, o konstrukcji cylindrycznej z umieszczoną w górnej części konstrukcją siatki osłonowej. Model górnej części komina wykonany w skali 1:19 został wyposażony w 3 poziomy punktów pomiarowych ciśnienia wiatru. Każdy poziom zawierał 24 punkty połączone ze skanerami ciśnienia. Na podstawie pomiarów ciśnienia wyznaczono średni i chwilowy współczynnik oporu aerodynamicznego oraz współczynniki siły bocznej. Następnie określono współczynniki porywów wiatru dla tych dwóch składowych działania wiatru. Ponadto dla każdego sygnału ciśnienia wykonano szybką transformację Fouriera. Średnie składowe siły działania wiatru zostały również określone przy użyciu wagi aerodynamicznej. Uzyskane wyniki pozwalają stwierdzić, że rozwiązanie zastosowane w górnej części projektowanego komina jest poprawne z punktu widzenia aerodynamiki budowli. Podczas badań modelowych górnej części komina praktycznie nie zaobserwowano wzbudzeń wirowych. Podstawowym wzbudzeniem dynamicznym tej części komina są turbulencje atmosferyczne.

Received: 2020-11-25, Revised: 2021-02-18